Detection using Block QR decomposition for MIMO HetNets

R. Thomas*, R. Knopp* B. T. Maharaj† and L. Cottatellucci*
*Mobile Communications Department, EURECOM, Biot, France
†Department of Electrical, Electronic and Computer Engineering, University of Pretoria, Pretoria, South Africa
Email:{robin.thomas, raymond.knopp, laura.cottatellucci}@eurecom.fr and sunil.maharaj@up.ac.za

***Abstract*—Interference management between uncoordinated eNBs and UEs is a crucial aspect of Heterogeneous Networks in LTE, especially if the interference can be exploited at the receiver. In this paper, a novel preprocessing Block QR decomposition technique is proposed for a low-complexity max-log-MAP receiver, for interference detection in a 4×4 HetNet scenario. The authors show that for various SNR, the proposed receiver detection scheme has minimal mutual information loss for Gaussian signals for the 4×4 and 8×8 case. The proposed preprocessing method is implemented in an LTE simulation test bench with practical codes and compared with a brute-force search max-log-MAP algorithm.**

I. Introduction

Wireless networks are on the verge of shifting towards heterogeneity by leveraging various radio access technologies, multiple access node types, etc. An example of a Heterogeneous Network (HetNet) could involve the deployment of multiple uncoordinated low powered nodes (eNBs) amidst existing coordinated infrastructure. As a consequence, User Equipments (UEs) may experience increased levels of inter-cell and intra-cell interference, due to numerous eNB deployments within a given area.

Inter-cell interference coordination techniques (ICIC) for LTE Rel-8/9 and enhanced-ICIC methods for LTE Rel-10 (LTE-A) have been included to resolve the interference issues experienced by HetNets [1]. Coordinated Multipoint (CoMP) transmission and reception strategies have also been defined for LTE Rel-11 and beyond, in order to exploit interference and improve the data rates and spectral efficiency of cell edge users [2]. Network-Assisted Interference Cancellation (NAIC) techniques have also been examined for LTE Rel-12, with design considerations for Interference Suppression (IS) and Cancellation (IC) receiver structures [3] also studied. As the name implies, IS techniques aim to suppress the effects of interference, e.g. Linear MMSE-IRC. IC approaches can either be performed on a codeword or symbol level, by consecutively stripping out the interference after each stage until the desired signal is remaining. Both IS and IC techniques require some degree of knowledge of the interferer.

In this paper, a novel preprocessing technique utlising Block QR decomposition for implementation in a low complexity max-log-MAP detection scheme has been proposed. This receiver is based on an interference awareness architecture presented in [4], which involves the exploitation of the dominant interferer affecting cell-edge users. Although this study, considers a HetNet scenario, the receiver front-end processing and detection method is also applicable to a point-to-point MIMO link and multi-user MIMO environments. In [5], a Blocking procedure has been used to partition the channel matrix to improve the packet error rate of a reduced-maximum likelihood detection technique, however in this case interference exploitation is absent. Block QR decomposition methods have also been studied as shown in [6] where the authors adapt the Dirty Paper Coding (DPC) scheme using Block QR decomposition to improve the performance of multi-user MIMO in the presence of intercell interference. The study of interference exploitation techniques at the receiver in the context of higher order MIMO HetNets has been limited. Initially, an information theoretic approach is undertaken to quantify the mutual information loss of the Block QR technique when compared to the 4×4 and 8×8 theoretical and MMSE case with Gaussian signal assumptions. These analytical results will be used as a reference to evaluate the performance of the proposed Block QR scheme with the suboptimal and more complex (brute-force search) max-log-MAP algorithm .

The paper is organised as follows. Section II is an overview of the system model, while Section III details the analytical expressions relating to the mutual information loss as well as the proposed Block QR decomposition technique. Section IV provides an overview of the two receiver architectures, i.e. the brute-force max-log-MAP algorithm and the reduced metric max-log-MAP algorithm with the proposed preprocessing, which has been implemented in a LTE simulation test bench. Section V examines the complexity and corresponding performance in terms of the frame error rate (FER), pertaining to the downlink simulations. Finally, Section VI concludes the paper.

II. System Model

An inter-cell interference setting for a femto UE is considered. This particular model (as noted in Fig. 1) consists of a downlink scenario where the UE is equipped with four receive antennas in the presence of two eNBs each equipped with two antennas, one of which is transmitting the desired signal, while the other is regarded as the interferer (macro-eNB). Conversely, the femto eNB could also be an interfering source to a macro UE. Moreover, this MIMO scenario can also be extended to an 8×8 system involving the deployment of a relay node equipped with eight antennas as opposed to a single UE (as noted later in Section III). The received signal ($\mathbf{y}_F$) in Fig. 1 can be represented in vector form by grouping the desired stream $\mathbf{s}_1$ and the interfering stream $\mathbf{s}_2$:

$$\mathbf{y}_F = \mathbf{H}\mathbf{s} + \mathbf{n}, \tag{1}$$

$$\begin{pmatrix} \mathbf{y}_1 \\ \mathbf{y}_2 \end{pmatrix} = \begin{pmatrix} \mathbf{H}_{11} & \mathbf{H}_{12} \\ \mathbf{H}_{21} & \mathbf{H}_{22} \end{pmatrix} \begin{pmatrix} \mathbf{s}_1 \\ \mathbf{s}_2 \end{pmatrix} + \begin{pmatrix} \mathbf{n}_1 \\ \mathbf{n}_2 \end{pmatrix}, \tag{2}$$

where the received signal is given by $\mathbf{y}_F = (\mathbf{y}_1\, \mathbf{y}_2)^T$ and each corresponding received signal is represented as $\mathbf{y}_1 = (r_1\, r_2)^T$ and $\mathbf{y}_2 = (r_3 r_4)^T$. The complex channel coefficients are given

as $(\mathbf{H}_{11}\ \mathbf{H}_{12}) \in \mathbb{C}^{N_{t1}\times N_r}$ and $(\mathbf{H}_{21}\ \mathbf{H}_{22}) \in \mathbb{C}^{N_{t2}\times N_r}$, where N_r represents the number of receive antennas, while N_{t1} and N_{t2} refers to the number of transmit antennas at each eNB. The spatially multiplexed transmit data from the femto and macro eNBs are given as $\mathbf{s}_1 = (x_1\ x_2)^T$ and $\mathbf{s}_2 = (x_3\ x_4)^T$, respectively (where the matrix transpose is given by $(.)^T$). The noise vectors, $\mathbf{n}_1$ and $\mathbf{n}_2$, are zero mean circularly symmetric complex Gaussian variables. The aim is to diagonalise the channel using a Block QR decomposition approach, such that the interfering signal is successfully decoded and thereafter stripped to obtain the desired signal using a technique such as SIC. This scheme enables the reduction of a 4×4 channel into 2×2 blocks. Similarly, in an an 8×8 system the channel would be divided into 4×4 blocks. The interference decoding is then performed using a low complexity max-log-MAP demodulator [4], [7], which was initially proposed for a 2×2 system. This model assumes that perfect channel state information (CSI) is available at the receiver.

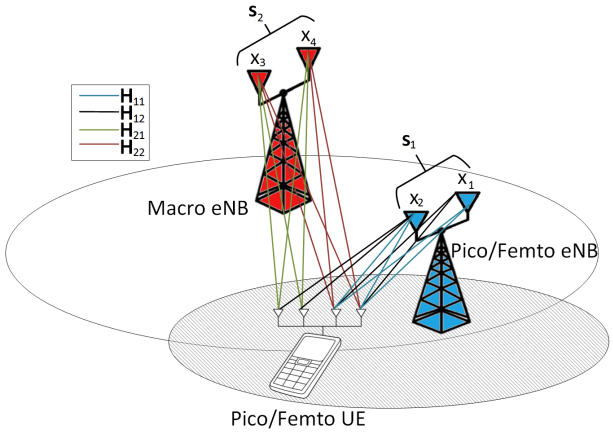

Figure 1. Basic HetNet model.

III. Mutual Information Analysis

The mutual information loss for the case of the Gaussian interferers' between the theoretical and Block QR scheme are initially analysed for a Rayleigh channel model (where ($\mathbf{s}_1$) and ($\mathbf{s}_2$) are the desired and interfering streams, respectively). The complete mutual information expression relating to Eq. (2) is:

$$I(\mathbf{s}_1, \mathbf{s}_2; \mathbf{y}_F|\mathbf{H}) = I(\mathbf{s}_2; \mathbf{y}_F|\mathbf{H}) + I(\mathbf{s}_1; \mathbf{y}_F|\mathbf{H}, \mathbf{s}_2), \quad (3)$$

where the mutual information, $I(\mathbf{s}_1, \mathbf{s}_2; \mathbf{y}_F|\mathbf{H})$, of the overall 4×4 model is defined as:

$$I(\mathbf{s}_1, \mathbf{s}_2, \mathbf{y}_F|\mathbf{H}) = \mathcal{H}(\mathbf{y}_F) - \mathcal{H}(\mathbf{y}_F|\mathbf{s}_1, \mathbf{s}_2), \quad (4)$$

and $\mathcal{H}\{.\}$ represents the signal entropy. The mutual information expression of the interferer is also given as:

$$I(\mathbf{s}_2; \mathbf{y}_F|\mathbf{H}) = \mathcal{H}(\mathbf{y}_F|\mathbf{H}) - \mathcal{H}(\mathbf{y}_F|\mathbf{H}, \mathbf{s}_2), \quad (5)$$

where the respective received signal entropies are:

$$\mathcal{H}(\mathbf{y}_F|\mathbf{H}) = \log_2\left\{\det\left(\pi e \mathbf{R}_{\mathbf{y}_F|\mathbf{H}}\right)\right\}, \quad (6)$$

$$\mathcal{H}(\mathbf{y}_F|\mathbf{H}, \mathbf{s}_2) = \log_2\left\{\det\left(\pi e \mathbf{R}_{\mathbf{y}_F|\mathbf{H},\mathbf{s_2}}\right)\right\}, \quad (7)$$

where $\mathbf{R}_{\mathbf{y}_F}$ and $\mathbf{R}_{\mathbf{y}_F|\mathbf{H},\mathbf{s_2}}$ represent the received signal covariance matrices. The mutual information loss between the theoretical (Eq. (4)) and the Block QR transformed interfering signal model are compared such that:

$$I(\mathbf{s}_1, \mathbf{s}_2; \mathbf{y}_F|\mathbf{H}) \geq I(\mathbf{s}_2; \tilde{\mathbf{y}}_2|\tilde{\mathbf{H}}) + I(\mathbf{s}_1; \tilde{\mathbf{y}}_F|\tilde{\mathbf{H}}, \mathbf{s}_2), \quad (8)$$

$$I(\mathbf{s}_2; \mathbf{y}_F|\mathbf{H} \geq I(\mathbf{s}_2; \tilde{\mathbf{y}}_\mathbf{2}|\tilde{\mathbf{H}})), \quad (9)$$

where the applied Block QR transformation on the received signal is given as $\tilde{\mathbf{y}}_F = (\tilde{\mathbf{y}}_\mathbf{1}\ \tilde{\mathbf{y}}_\mathbf{2})^T$ while $\tilde{\mathbf{H}}$ is the equivalent Block QR decomposed channel matrix (detailed in Section III-A). This loss can be examined by studying the outage probabilities especially around 10^{-1}, where in the case of LTE, is an acceptable level of outage for the initiation of the Hybrid-ARQ protocol [8].

A. Block QR Decomposition

Blocking algorithms generally tend to work on multiple columns and rows simultaneously and has served as an efficient way to perform matrix computations on hierarchical memory structures. A recursive Block QR factorization has been developed, which partitions the target matrix into a series of blocks and has been validated through mathematical induction [9], [10]. According to [9], elementary Householder transformations are used to factorize the last remaining column and in the process, inherently stops the recursion. The transformed received signal based on Eq. (1) is expressed as:

$$\mathbf{y}_F = \mathbf{Q}_1\mathbf{Q}_2\mathbf{R}\mathbf{s} + \mathbf{n}, \quad (10)$$

where $\mathbf{Q}_1$ and $\mathbf{Q}_2$ are orthogonal matrices and are partitioned into blocks as follows:

$$\mathbf{Q}_1 = \begin{pmatrix} \mathbf{Q}_{11} & \mathbf{Q}_{12} \\ \mathbf{Q}_{21} & \mathbf{Q}_{22} \end{pmatrix}; \mathbf{Q}_2 = \begin{pmatrix} \mathbf{I} & \mathbf{0} \\ \mathbf{0} & \tilde{\mathbf{Q}}_2 \end{pmatrix}, \quad (11)$$

where the $N_t \times N_r$ channel matrix (N_t and N_r denotes the total number of transmit and receive antennas, respectively) has been partitioned into $k\times k$ blocks, where $k = 2$ and $k = 4$ for the 4×4 and 8×8 cases, respectively. It should be also noted that $N_t = N_r = 2^p$ for $p > 1$, where p is the blocking order for the square channel matrix. The upper triangular matrix $\mathbf{R}$ is also block partitioned as follows:

$$\mathbf{R} = \begin{pmatrix} \mathbf{R}_{11} & \mathbf{R}_{12} \\ \mathbf{0} & \mathbf{R}_{22} \end{pmatrix}. \quad (12)$$

The transformed received signal is:

$$\tilde{\mathbf{y}}_F = \tilde{\mathbf{H}}\mathbf{s} + \tilde{\mathbf{n}}, \quad (13)$$

where $\tilde{\mathbf{y}}_F = \mathbf{Q}_1^T\mathbf{y}_F$, $\tilde{\mathbf{H}} = \mathbf{Q}_2\mathbf{R}$, $\tilde{\mathbf{n}} = \mathbf{Q}_1^T\mathbf{n}$ and also $\tilde{\mathbf{Q}}_2 = \mathbf{R}_{22}\tilde{\mathbf{H}}_{22}$, given that:

$$\mathbf{Q}_1^T\mathbf{H} = \begin{pmatrix} \mathbf{R}_{11} & \mathbf{R}_{12} \\ \mathbf{0} & \tilde{\mathbf{H}}_{22} \end{pmatrix}. \quad (14)$$

Householder transformations are initially computed to determine the orthogonal $\mathbf{Q}$ and upper-triangular $\mathbf{R}$ matrix. Alternatively, the Givens rotations QR factorization technique can also be utilised, with comparable performance while only differing in algorithmic complexity.

B. Analytical Results

The cumulative distribution functions (CDFs) for the maximal achievable rate for the different SNR values are examined for the theoretical, Block QR and MMSE cases. Figs. 2 and 3 represent the theoretical CDF curves for the 4×4 (two interfering streams) and 8×8 (four interfering streams) channels, respectively. For an outage probability of 10^{-1} and at an SNR of 15 dB the achievable rate difference for the 4×4 model between the Block QR and theoretical case is 0.55 bits/s/Hz, while for an SNR of 25 dB, the difference reduces to 0.3 bits/s/Hz. As a result, the Block QR scheme approaches the theoretical limit at higher SNRs, while the MMSE rate degrades rapidly for the detection of the target interferer, which is especially prominent in the 8×8 case as noted in Fig. 3. It must be noted that statistics of the channel are Rayleigh

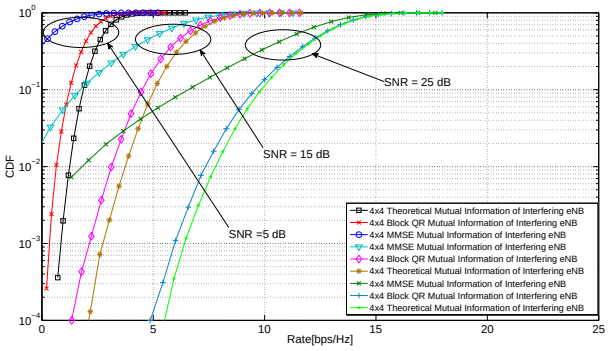

Figure 2. Mutual Information loss at various SNR for the 4×4 MIMO model.

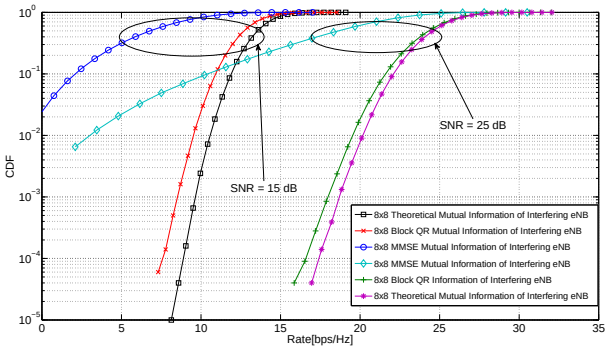

Figure 3. Mutual Information loss at various SNR for the 8×8 MIMO model.

with equal power allocation at the transmitter. Moreover, the Householder transformation QR decomposition method was selected for the Block algorithm to generate the Block QR CDFs in Figs. 2 and 3. The aforementioned theoretical results are then studied with respect to the implementation in a simulation test bench, based on the OpenAirInterface simulator [11]. This would involve a comparative performance evaluation of the LTE physical layer downlink simulation of the low-complex max-log-MAP detector [4], [7] and suboptimal brute-force search max-log-MAP detector [12] (see Section V-C). The simulation of an 8×8 system is out of the scope of this study since a new soft-decision metric has to be developed for the four stream interferer, in order to exploit the statistics to aid in the decoding of the desired four streams.

IV. Receiver Architectures

UEs can exploit the interference from surrounding sources in an interference limited environment, as opposed to simply nulling out the interference. In this case, low-complexity detection algorithms are highly desirable especially for MIMO receivers. Brute-force maximum-likelihood (ML) is a well-known to be the optimal detection technique in terms of performance with prohibitively high complexity based on the number of antennas and modulation order. The reduced metric max-log-MAP detector developed in [4] for Bit Interleaved Coded Modulation (BICM) systems aims to lower complexity by reducing the search space by one complex dimension through the ordering of the real and imaginary components of the matched filter outputs. The aforementioned two detection techniques will be discussed in relation to a 4×4 scenario, described by Eq. 2.

A. Max-log-MAP Approximation

In the case of a ML receiver, the objective is to maximise the probability of correct symbol detection for the interfering stream, $\mathbf{s}_2$ (equivalent to minimising the euclidean distance between the received symbol vector and the set of all transmitted symbol vectors), the hard-decision is then expressed as:

$$\hat{\mathbf{s}}_2 = \max_{\mathbf{s} \in M_q} \{P(\mathbf{y}_F|\mathbf{s})\} = \min_{\mathbf{s} \in M_q} \|\mathbf{y}_F - \mathbf{H}\mathbf{s}\|^2, \qquad (15)$$

where M_q is the set of discrete complex symbol points. For equally likely bits, the log-likelihood ratio (LLR) is a soft-decision based metric and is computed using on the max-log approximation:

$$\lambda_{k,i} = \min_{s \in \chi^0_{k,i}} \|\mathbf{y}_F - \mathbf{H}\mathbf{s}\|^2 - \min_{s \in \chi^1_{k,i}} \|\mathbf{y}_F - \mathbf{H}\mathbf{s}\|^2, \qquad (16)$$

where $k = 1, ..., N_r \log_2 M_q$ represents the bit position of interest on the i^{th} stream, N_r being the number of receive antennas, while χ^0_k and χ^1_k are sets of equal size representing all possible constellation points, where the k^{th} bit of interest is 0 or 1, respectively. Alternatively, the bit metric is equivalently expressed as a maximization problem:

$$\lambda_k = \max_{x_3, x_4 \in M_q} \left\{ - \|\mathbf{y}_F - \mathbf{H}\mathbf{s}\|^2 \right\}. \qquad (17)$$

The max-log approximation remains a suboptimal algorithm when compared to the true MAP detection algorithm [12].

B. Reduced Metric MAP Receiver

A spatial interference cancellation technique has been proposed for a MIMO cell edge users, where a simplified bit metric based on the max-log-MAP detector in Eq. (16) has been developed for discrete constellations. The proposed technique is low in complexity as it reduces the overall search space by one complex dimension and the results show that the frame error rate (FER) performance improves as the strength of the interferer increases for QPSK, 16 QAM and 64 QAM constellations [4], [7]. The low-complexity approximation is based on the decoupling of the real and imaginary components and the computation of the matched filter (MF) output. Expanding

$$\lambda = \max_{\substack{x_3 \in M_q \\ x_4 \in M_q}} \{ - \|\mathbf{h}_a\|^2 |x_3|^2 - \|\mathbf{h}_b\|^2 |x_4|^2 + 2 [\Re\{\bar{r}_3\}\Re\{x_3\} + \Im\{\bar{r}_3\}\Im\{x_3\}] - 2\eta_0 \Re\{x_4\} - 2\eta_1 \Im\{x_4\} \}. \quad (21)$$

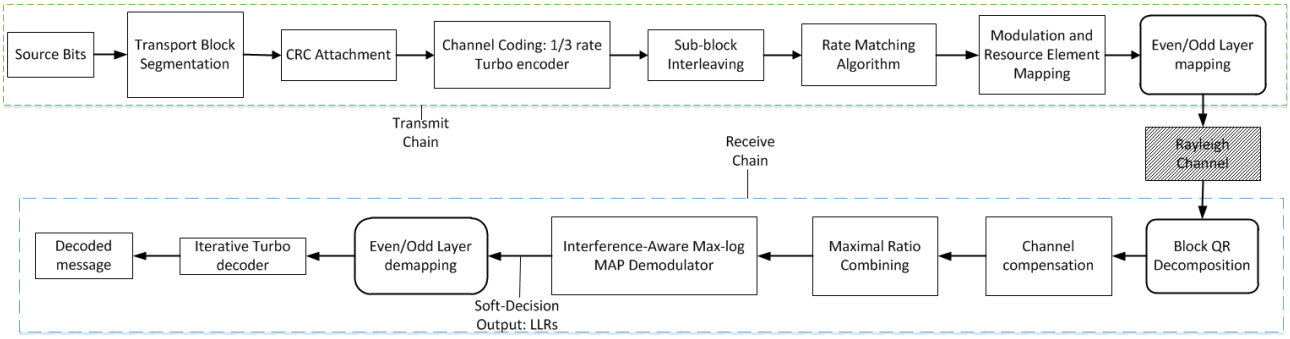

Figure 4. Overall simulation block diagram.

upon Eq. (16) and grouping the real and imaginary components, results in the development of the reduced LLR bit metric (λ) as seen in Eq. (21), where the matched filtered output of the interfering signal is $\bar{\mathbf{y}}_2 = (\tilde{\mathbf{H}}_{22})^T \tilde{\mathbf{y}}_2 = (\bar{r_3}\, \bar{r_4})$ and the column block channel vectors are given by $\tilde{\mathbf{H}}_{22} = (\mathbf{h}_a\, \mathbf{h}_b)$, while $\Re\{.\}$ and $\Im\{.\}$ represent the real and imaginary components of the particular signal. The terms η_0 and η_1 are given as [4], [7]:

$$\eta_0 = \Re(\rho_{ab})\Re(x_3) + \Im(\rho_{ab})\Im(x_3) - \Re(\bar{r}_4), \quad (18)$$

$$\eta_1 = \Re(\rho_{ab})\Im(x_3) - \Im(\rho_{ab})\Re(x_3) - \Im(\bar{r}_4), \quad (19)$$

where $\rho_{ab} = (\mathbf{h}_a^T \mathbf{h}_b)$, is the correlation coefficient between the interfering streams. For this study, the modulation order (M_q) of the desired and interfering signal is assumed to be the same, i.e. QPSK.

V. Complexity and Performance

A. Recursive Block QR Complexity

The Block QR algorithm provides a more flexible approach to blocking, as it uses a divide-and-conquer approach to perform the decomposition. This algorithm is well suited for parallel computations since it is largely based on matrix multiplications. It should be noted that the analysed complexity is applicable to a 4×4 (square) matrix according to this particular scenario. In terms of the analysis, n is denoted as the number of floating operations (flops) within the algorithm. The time complexity is given as:

$$T(n) = 2\log_{\frac{N_r}{k}} n + 2n^3 + 19, \quad (20)$$

where $N_r = 4$ and $k = 2$ represents the block size (as defined in Section III-A). Therefore, an additional complexity of $2n^3 + 2\log_2 n + 19$ operations is introduced due to the recursive Block QR decomposition algorithm for the 4×4 model.

B. Simulation Model

The performance evaluations of the proposed Block QR decomposition technique are validated using the OpenAirInterface software platform [13]. This platform serves as an open source hardware and software development framework, which among many features, includes the end-to-end experimentation of the physical layer uplink and downlink channels in accordance with the 3GPP LTE specifications. In this particular scenario, the baseband simulations are carried out on the LTE downlink-shared channel (DL-SCH), which is essentially responsible for the transmission of user pertinent information to the higher layers (including control information) in the protocol stack. Fig. 4 shows the physical layer processing blocks implemented in the LTE simulation test bench. Messages in LTE are transmitted in the form of Transport Blocks, where error detection is enabled by appending 24 Cyclic Redundancy Check (CRC) bits at the end of each transport block. The Transport Block Size (TBS) depends on the Modulation and Coding Scheme (MCS), which characterises the modulation order and coding rate of a codeword and can be referenced from a lookup table depending on the number of transmitted layers [14]. In an LTE transmission, a maximum of 2 codewords can only be transmitted in order to achieve the balance between receiver processing (including signaling requirements of CQI and H-ARQ) and performance. Therefore, in the case of a 4×4 MIMO system, the modulated symbols of the 2 codewords are mapped according to layers using a grouping of even and odd symbols. In this case, each codeword is mapped onto 2 layers, providing a total of transmission of 4 layers. The LTE channel codes consists of a 1/3 rate Turbo encoder, which follows the structure of a parallel concatenated convolutional code with two 8-state constituent encoders and one turbo code internal interleaver [15]. During channel compensation, the matched filter channel outputs are obtained in addition to the scaled channel magnitudes. The compensated signals are combined using the maximal ratio combining (MRC) technique [16] and thereafter, the soft-decision outputs of the interferer are obtained using the two demodulators (brute-force search and reduced metric max-log-MAP algorithms). The LLRs are then demapped for decoding by the iterative turbo decoder. Table I outlines the key simulation parameters.

C. Performance

The FER performances have been simulated for the moderate to higher SNR regimes for both the sub-optimal exhaustive max-log-MAP and Block QR receiver algorithms in an LTE scenario. Fig. 5 shows the corresponding performance for QPSK (MCS=9) signals for both practical demodulators. Fur-

Table I. SIMULATION SPECIFICATIONS

Parameter	Value
Transmission Mode	4
Channel Bandwidth	5 MHz
Number of Resource Blocks	50
Modulation and Coding Scheme	9
Channel Coding	1/3 rate Turbo encoder
Channel Type	Rayleigh
Transport Block Size (4 layers)	7992

thermore, the same plot (Fig. 5) also shows the outage as a function of SNR at a fixed rate corresponding to the 10^{-1} outage probability of the interfering eNB for the theoretical and proposed Block QR 4×4 schemes. The Householder transformation technique was implemented to perform the QR decomposition.

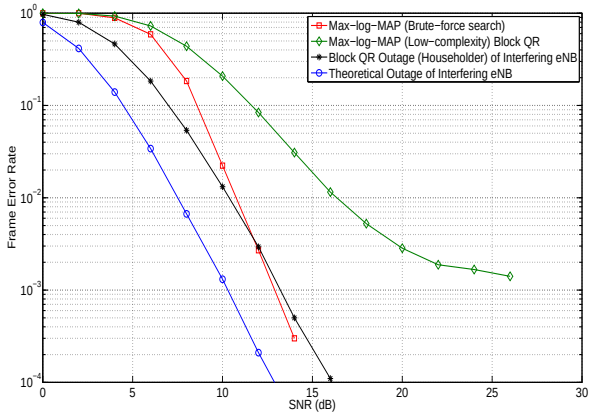

Figure 5. FER performance between the low-complex Block QR max-log-MAP and Brute-force max-log-MAP search algorithm using LTE practical codes

The difference between the two analytical outage schemes (theoretical (blue) and Block QR (black) curves) and the two practical demodulators (brute-force (red) and Block QR max-log-MAP (green) curves) at 10^{-1} is 2.5 dB and 3 dB, respectively. Moreover, the diversity order can also be compared between theory and practice. It can be noted that the theoretical and brute-force search max-log-MAP scheme display a similar diversity of 4, while the practical Block QR FER performance has a diversity order of 2. It was observed that the Block QR max-log-MAP demodulator was significantly less complex in terms of simulation time (hours) when compared to the brute-force search max-log-MAP algorithm by a factor of approximately 12. This supports the feasibility of such a scheme in future advanced receivers for NAIC.

VI. CONCLUSIONS

A novel channel preprocessing MIMO detection scheme based on a recursive Block QR decomposition approach for a single-user HetNet scenario has been proposed. This technique exploits the low-complexity max-log-MAP algorithm, to perform interference detection for higher order MIMO receivers. The corresponding information theoretic results show that for the 4×4 and 8×8 MIMO channels, the mutual information loss between the theoretical and Block QR outage probability is minimal, for Gaussian signals. Furthermore, the proposed Block QR scheme is validated in a practical scenario, using a simulation test bench based on a full LTE downlink physical layer scenario with discrete constellations. The practical results reveal the feasibility of the Block QR approach for NAIC receivers. Future work, will focus on obtaining throughput performance curves for the Block QR decomposition approach for all MCS values including higher order modulation orders (16 QAM and 64 QAM) as well as the performance evaluation of SIC for the perfect and imperfect channel estimation cases.

VII. ACKNOWLEDGMENTS

EURECOM's research is partially supported by its industrial members: BMW Group Research and Technology, IABG, Monaco Telecom, Orange, SAP, SFR, ST Microelectronics and Symantec. This research work is also partially supported by the National Research Foundation (NRF) of South Africa.

REFERENCES

[1] D. Lopez-Perez, I. Guvenc, G. de la Roche, M. Kountouris, T. Quek, and J. Zhang, "Enhanced intercell interference coordination challenges in heterogeneous networks," *IEEE Wireless Commun.*, vol. 18, no. 3, pp. 22–30, Jun. 2011.

[2] R. Irmer, H. Droste, P. Marsch, M. Grieger, G. Fettweis, S. Brueck, H. P. Mayer, L. Thiele, and V. Jungnickel, "Coordinated multipoint: Concepts, performance, and field trial results," *IEEE Commun. Mag.*, vol. 49, no. 2, pp. 102–111, Feb. 2011.

[3] Third Generation Partnership Project, "Study on Network-Assisted Interference Cancellation and Suppression (NAIC) for LTE (Release 12)," 3GPP, Tech. Rep. 3GPP TR 36.866 v12.0.0, Mar. 2014.

[4] R. Ghaffar and R. Knopp, "Interference Suppression for Next Generation Wireless Systems," in *IEEE VTC Spring 2009.*, Apr. 2009, pp. 1–5.

[5] S. Kinjo, A. Liu, and S. Ohno, "A study on reduced MLD utilizing the QR decomposition for MIMO communication systems," in *Intl. Conf. on Green Circuits and Systems (ICGCS)*, Jun. 2010, pp. 259–262.

[6] A. Yousafzai and M. Nakhai, "Block QR decomposition and near-optimal ordering in intercell cooperative MIMO-OFDM," *IET Commun.*, vol. 4, no. 12, pp. 1452–1462, Aug. 2010.

[7] R. Ghaffar and R. Knopp, "Spatial Interference Cancellation Algorithm," in *IEEE WCNC*, Apr. 2009, pp. 1–5.

[8] P. Wu and N.Jindal, "Coding versus ARQ in Fading Channels: How reliable should PHY be? ," *IEEE Trans. on Commun.*, vol. 59, no. 12, pp. 3363–3374, Dec. 2011.

[9] E. Elmroth and F. Gustavson, "Applying recursion to serial and parallel QR factorization leads to better performance," *IBM J. RES. DEVELOP.*, vol. 44, no. 4, pp. 605–624, Jul. 2000.

[10] G. H. Golub and C. F. V. Loan, *Matrix Computations*, 4th ed. John Hopkins University Press, 2013.

[11] F. Kaltenberger, "OpenAirInterface Project," Eurecom, Feb. 2014, https://twiki.eurecom.fr/twiki/bin/view/OpenAirInterface. Last accessed on 23 Nov. 2014.

[12] P. Robertson, E. Villebrun, and P. Hoeher, "A comparison of optimal and sub-optimal MAP decoding algorithms operating in the log domain," in *IEEE Intl. Conf. on Commun. (ICC)*, vol. 2, Jun. 1995, pp. 1009–1013.

[13] F. Kaltenberger, R. Ghaffar, R. Knopp, H. Anouar, and C. Bonnet, "Design and Implementation of a Single-frequency Mesh Network Using OpenAirInterface," *EURASIP J. Wirel. Commun. Netw.*, vol. 2010, no. 19, pp. 1–12, Apr. 2010.

[14] Third Generation Partnership Project, "Phyisical Layer Procedures (Release 11)," 3GPP, Tech. Rep. 3GPP TS 36.213 v11.3.0, Jun. 2013.

[15] ——, "Multiplexing and channel coding (Release 11)," 3GPP, Tech. Rep. 3GPP TS 36.212 v11.3.0, Jun. 2013.

[16] C. Johnson, *Long Term Evolution in Bullets*, 1st ed. CreateSpace Independent, 2010.